SC primary tumors showed no difference in size (Fig. 6B,C). Furthermore, although imatinib mesylate treatment had little effect on the size of primary SC tumors, it significantly suppressed lung metastasis in primary tumors (Fig. 6C). These data suggest that $CD90^+$ cells are not only metastatic to the distant organ, but also help the metastasis of $CD90^-$ cells, including $EpCAM^+$ cells, which originally have no distant metastatic capacity. Our data further suggest that imatinib mesylate can inhibit distant organ metastasis by suppressing $CD90^+$ metastatic CSCs, albeit with little effect on $EpCAM^+$ tumorigenic epithelial stem-like CSCs.

To explore the potential mechanism of how $CD90^+$ cells dictate the metastasis of $EpCAM^+$ cells, we utilized coculture systems and time-lapse image analysis. Wound-healing analysis clearly indicated that motility of HuH7 cells was enhanced when HLF cells were cocultured, and this effect was abolished by imatinib mesylate treatment (Fig. 6D; see Supporting Videos 1-3). HLF cells abundantly expressed *TGFB1*, compared with HuH7 cells, and its expression was dramatically suppressed by imatinib mesylate treatment (Fig. 6E). Mothers against decapentaplegic homolog 3 (Smad3) phosphorylation was augmented in HuH7 cells when cocultured with HLF cells, and this effect was attenuated when cocultured with HLF cells pretreated with imatinib mesylate.

Taken together, our data suggest that liver CSCs are not a single entity. Liver CSCs defined by different markers show unique features of tumorigenicity/metastasis with phenotypes closely associated with committed liver lineages. These distinct CSCs may collaborate to enhance tumorigenicity and metastasis of HCCs.

Discussion

The current investigation demonstrates that CSC marker expression status may be a key determinant of cancer phenotypes, in terms of metastatic propensity and chemosensitivity, to certain molecularly targeted therapies. EpCAM appears to be an epithelial tumorigenic CSC marker, whereas CD90 seems to be a mesenchymal metastatic CSC marker associated with expression of c-Kit and chemosensitivity to imatinib mesylate. Imatinib mesylate may be effective in inhibiting metastasis, but has little effect on primary $EpCAM^+$ HCC cell growth.

We investigated the frequency of three CSC markers (EpCAM, CD90, and CD133) in 15 primary HCCs with a confirmed cell viability of $\geq$70% and found that three HCCs contained $CD133^+$ cells, seven HCCs contained $EpCAM^+$ cells, and all HCCs contained $CD90^+$ cells. Among them, we confirmed the perpetuation of $CD133^+$ cells derived from three HCCs (P7, P12, and P14; data not shown), $EpCAM^+$ cells derived from four HCCs (P4, P7, P13, and P14), and $CD90^+$ cells derived from two HCCs (P12 and P15). Recent studies showed that at least 8 of 21 HCCs (38%)[4] and 13 of 13 HCCs (100%)[5] contained tumorigenic $CD133^+$ or $CD90^+$ CSCs, respectively. Recent IHC and tissue microarray studies also demonstrated that $CD133^+$ and $CD90^+$ cells were detected in 24.8% ($\geq$1% of tumor cells) and 32.2% ($\geq$5% of tumor cells) of HCC cases examined, respectively.[15,16]

One possible explanation of the comparatively low frequency of $CD133^+$ liver CSCs identified in our study is that we used the monoclonal Ab CD133/2, whereas Ma et al. used CD133/1. Another possible explanation is the difference of etiology related to hepatocarcinogenesis. We examined tumorigenicity using 15 HCCs (five HBV related, four HCV related, three non-B, non-C hepatitis [NBNC] related, and three alcohol related) and identified that tumorigenic CSCs were only obtained from HBV- or HCV-related cases. Previous liver CSC studies were performed using HBV-related HCCs,[4,5] and a recent study showed that

Fig. 6. Suppression of lung metastasis mediated by $CD90^+$ CSCs by imatinib mesylate. (A) FACS analysis of seven HCC cell lines stained by APC-CD105, Alexa 488/VEGFR1, APC/VEGFR2, and Alexa 488/c-Kit Abs or isotype control. (B) Tumorigenicity of 5×10^5 HuH7 cells and 2.5×10^5 HuH7 cells plus 2.5×10^5 HLF cells treated with imatinib mesylate or control phosphate-buffered saline (PBS) (200 μL/mouse) orally ingested three times per week (100 mg/kg) for 2 weeks. Data are generated from 5 mice per condition. (C) IHC analysis of EpCAM in lung metastasis detected in NOD/SCID mice SC injected with 2.5×10^5 HuH7 cells and 2.5×10^5 HLF cells. Metastasis was evaluated macro- and microscopically in the left and right lobes of the lung separately in each mouse ($n = 5$) (scale bar, 100 μm). (D) Cell motility of HuH7 cells cocultured with HuH7, HLF, or HLF cells with imatinib mesylate (10 μM) was monitored in a real-time manner by time-lapse image analysis. HuH7 and HLF cells were labeled with the lipophilic fluorescence tracer, DiI (indicated as red) or DiD (indicated as blue), and incubated in a μ-Slide eight-well chamber overnight. Silicone inserts were detached and the culture media replaced with Dulbecco's modified Eagle's medium containing 10% fetal bovine serum, including 0.1% dimethyl sulfoxide (DMSO) (control) or 10 μM of imatinib mesylate dissolved in DMSO (final concentration 0.1%). Immediately after the medium change, cells were cultured at 37°C in 5% CO_2 and time-lapse images were captured for 72 hours. (E) qPCR analysis of *TGFB1* in HuH7 (white bar), HLF (gray bar), and HLF cells pretreated with imatinib mesylate for 24 hours. (F) Smad3 and its phosphorylation evaluated by western blotting. HuH7 cells and HLF cells were harvested in cell culture inserts and treated with DMSO (0.1%) or imatinib mesylate (10 μM) for 24 hours. Cell culture inserts were washed with PBS, cocultured with HuH7 cells for 8 hours, and then removed. HuH7 cells were lysed using radioimmunoprecipitation assay buffer for western blotting. (A) HuH7 cells cocultured with HuH7 cells. (B) HuH7 cells cocultured with HLF cells. (C) HuH7 cells cocultured with HLF cells pretreated with imatinib mesylate.

HBV X may play a role in generating $EpCAM^+$ CSCs.[17] The role of hepatitis virus infection on the generation of CSCs is still unclear and should be clarified in future studies.

We were unable to confirm the tumorigenicity of $CD90^+$ cells in 13 of 15 HCCs, but we observed abundant $CD90^+$ cells in more-advanced HCCs by IHC (data not shown). Tumorigenic $CD90^+$ cells may emerge at a later stage of hepatocarcinogenesis, and the majority of $CD90^+$ cells in early HCCs may be cancer-associated VECs without tumorigenic capacity. Furthermore, we identified tumorigenic $CD90^+$ cells only from HBV-related HCCs, and a recent study suggested that expression of CD90 was associated with HBV infection.[16] We could not detect the small population of $CD90^+$ HuH7 and Hep3B cells reported on by Yang et al. However, because we identified a small population of $CD90^+$ HuH7 cells after treatment with 5-FU (manuscript in preparation), it is conceivable that different cellular stress statuses may explain the observed differences between our findings and those of Yang et al.

The majority of CSC markers discovered thus far are almost identical to those found in healthy tissue stem cells or embryonic stem cells. However, with regard to the liver, the characteristics of healthy hepatic stem/progenitor cells isolated using different stem cell markers are currently under investigation. A recent article examined the characteristics of $EpCAM^+$ and $CD90^+$ oval cells isolated from 2-acetylaminofluorene/partial hepatectomy or D-galactosamine-treated rats.[18] Interestingly, $EpCAM^+$ and $CD90^+$ oval cells represent two distinct populations: The former expresses classical oval cell markers, such as AFP, OV-1, and cytokeratin-19 (CK-19), whereas the latter expresses desmin and alpha smooth muscle actin, but not AFP, OV-1, or CK-19, which indicates that $CD90^+$ populations are more likely to be mesenchymal cells. Another study has demonstrated that mesenchymal cells can interact with HSCs to regulate cell-fate decision.[19] We found that $EpCAM^+$ and $CD90^+$ cells isolated from liver cancer are distinct in terms of gene- and protein-expression patterns in both primary liver cancers and cell lines. Furthermore, these distinct CSCs can interact to regulate the tumorigenicity and metastasis of HCC. Molecular characteristics of $EpCAM^+/CD90^+$ CSCs may potentially reflect the cellular context of healthy stem or progenitor cells.

Although our study strongly indicates that abundant $CD90^+$ cells in a tumor is a risk for distant metastasis in liver cancer, the cell identity and role of $CD90^+$ cells remains elusive. As our IHC, FACS, and xeno-transplantation assays revealed, some $CD90^+$ cells in liver cancer may be cancer-associated VECs or fibroblasts that cannot perpetuate in the xenograft. Recent findings have suggested the importance of stromal cells in tumorigenesis and cancer metastasis,[20-22] so it is possible that these cells may help TECs invade and intravasate into blood vessels, thus playing crucial roles in metastasis.

Another possibility is that $CD90^+$ cells are cancer cells with features of fibroblasts (having undergone EMT) or VECs (having undergone vasculogenic mimicry; VM) that can invade, intravasate, and metastasize cells to distant organs. Recently, two groups reported that a subset of tumor VECs originate from glioblastoma CSCs.[23,24] We successfully confirmed the tumorigenicity and metastatic capacity of $CD90^+$ cells that were morphologically identical to VECs from primary HCCs that could perpetuate in the xenograft. However, a recent study demonstrated that $CD90^+$ HCC cells express glypican-3, a marker detected in hepatic epithelial cells.[25] Further studies are warranted to clarify the nature and role of $CD90^+$ HCC cells.

In our study, $CD90^+$ cells expressed the endothelial marker, c-Kit, CD105, and VEGFR1, and a mesenchymal VEC morphology and high metastatic capacity were confirmed in both primary liver cancer and cell lines. We further confirmed that $CD90^+$ liver cancer cells showed chemosensitivity to imatinib mesylate, suggesting that cancer cells committed to mesenchymal endothelial lineages could be eradicated by the compound. Although imatinib mesylate treatment had little effect on the size of primary tumors originated from both $EpCAM^+$ and $CD90^+$ CSCs, it significantly suppressed lung metastasis *in vivo*. These data are consistent with a recent phase II study demonstrating the tolerable toxicity, but limited efficacy, of imatinib mesylate alone for unresectable HCC patients. Eligibility of imatinib mesylate for advanced HCC patients may be restricted to the HCC subtypes organized by $CD90^+$ CSCs with a highly metastatic capacity and VEC features. Therefore, a combination of compounds targeting $EpCAM^+$ tumorigenic CSCs as well as $CD90^+$ metastatic CSCs may be required for the eradication of HCC and should be tested in the future.

Acknowledgments: The authors thank Ms. Nami Nishiyama and Ms. Mikiko Nakamura for their excellent technical assistance.

References

1. Tsai WL, Chung RT. Viral hepatocarcinogenesis. Oncogene 2010;29: 2309-2324.

2. Chiba T, Kita K, Zheng YW, Yokosuka O, Saisho H, Iwama A, et al. Side population purified from hepatocellular carcinoma cells harbors cancer stem cell-like properties. HEPATOLOGY 2006;44:240-251.
3. Haraguchi N, Ishii H, Mimori K, Tanaka F, Ohkuma M, Kim HM, et al. CD13 is a therapeutic target in human liver cancer stem cells. J Clin Invest 2010;120:3326-3339.
4. Ma S, Tang KH, Chan YP, Lee TK, Kwan PS, Castilho A, et al. miR-130b promotes CD133(+) liver tumor-initiating cell growth and self-renewal via tumor protein 53-induced nuclear protein 1. Cell Stem Cell 2010;7:694-707.
5. Yang ZF, Ho DW, Ng MN, Lau CK, Yu WC, Ngai P, et al. Significance of CD90+ cancer stem cells in human liver cancer. Cancer Cell 2008;13:153-166.
6. Zen Y, Fujii T, Yoshikawa S, Takamura H, Tani T, Ohta T, Nakanuma Y. Histological and culture studies with respect to ABCG2 expression support the existence of a cancer cell hierarchy in human hepatocellular carcinoma. Am J Pathol 2007;170:1750-1762.
7. Lee TK, Castilho A, Cheung VC, Tang KH, Ma S, Ng IO. CD24(+) liver tumor-initiating cells drive self-renewal and tumor initiation through STAT3-mediated NANOG regulation. Cell Stem Cell 2011;9: 50-63.
8. Yamashita T, Budhu A, Forgues M, Wang XW. Activation of hepatic stem cell marker EpCAM by Wnt-beta-catenin signaling in hepatocellular carcinoma. Cancer Res 2007;67:10831-10839.
9. Yamashita T, Forgues M, Wang W, Kim JW, Ye Q, Jia H, et al. EpCAM and alpha-fetoprotein expression defines novel prognostic subtypes of hepatocellular carcinoma. Cancer Res 2008;68:1451-1461.
10. Yamashita T, Ji J, Budhu A, Forgues M, Yang W, Wang HY, et al. EpCAM-positive hepatocellular carcinoma cells are tumor-initiating cells with stem/progenitor cell features. Gastroenterology 2009;136: 1012-1024.
11. Ma S, Chan KW, Hu L, Lee TK, Wo JY, Ng IO, et al. Identification and characterization of tumorigenic liver cancer stem/progenitor cells. Gastroenterology 2007;132:2542-2556.
12. Heffelfinger SC, Hawkins HH, Barrish J, Taylor L, Darlington GJ. SK HEP-1: a human cell line of endothelial origin. In Vitro Cell Dev Biol 1992;28A:136-142.
13. Ishimoto T, Nagano O, Yae T, Tamada M, Motohara T, Oshima H, et al. CD44 variant regulates redox status in cancer cells by stabilizing the xCT subunit of system xc(-) and thereby promotes tumor growth. Cancer Cell 2011;19:387-400.
14. Ramadori G, Fuzesi L, Grabbe E, Pieler T, Armbrust T. Successful treatment of hepatocellular carcinoma with the tyrosine kinase inhibitor imatinib in a patient with liver cirrhosis. Anticancer Drugs 2004;15: 405-409.
15. Kim H, Choi GH, Na DC, Ahn EY, Kim GI, Lee JE, et al. Human hepatocellular carcinomas with "Stemness"-related marker expression: keratin 19 expression and a poor prognosis. HEPATOLOGY 2011;54: 1707-1717.
16. Lu JW, Chang JG, Yeh KT, Chen RM, Tsai JJ, Hu RM. Overexpression of Thy1/CD90 in human hepatocellular carcinoma is associated with HBV infection and poor prognosis. Acta Histochem 2011;113: 833-838.
17. Arzumanyan A, Friedman T, Ng IO, Clayton MM, Lian Z, Feitelson MA. Does the hepatitis B antigen HBx promote the appearance of liver cancer stem cells? Cancer Res 2011;71:3701-3708.
18. Yovchev MI, Grozdanov PN, Zhou H, Racherla H, Guha C, Dabeva MD. Identification of adult hepatic progenitor cells capable of repopulating injured rat liver. HEPATOLOGY 2008;47:636-647.
19. Wang Y, Yao HL, Cui CB, Wauthier E, Barbier C, Costello MJ, et al. Paracrine signals from mesenchymal cell populations govern the expansion and differentiation of human hepatic stem cells to adult liver fates. HEPATOLOGY 2010;52:1443-1454.
20. Dome B, Timar J, Ladanyi A, Paku S, Renyi-Vamos F, Klepetko W, et al. Circulating endothelial cells, bone marrow-derived endothelial progenitor cells and proangiogenic hematopoietic cells in cancer: from biology to therapy. Crit Rev Oncol Hematol 2009;69:108-124.
21. Karnoub AE, Dash AB, Vo AP, Sullivan A, Brooks MW, Bell GW, et al. Mesenchymal stem cells within tumour stroma promote breast cancer metastasis. Nature 2007;449:557-563.
22. Mishra PJ, Humeniuk R, Medina DJ, Alexe G, Mesirov JP, Ganesan S, et al. Carcinoma-associated fibroblast-like differentiation of human mesenchymal stem cells. Cancer Res 2008;68:4331-4339.
23. Ricci-Vitiani L, Pallini R, Biffoni M, Todaro M, Invernici G, Cenci T, et al. Tumour vascularization via endothelial differentiation of glioblastoma stem-like cells. Nature 2010;468:824-828.
24. Wang R, Chadalavada K, Wilshire J, Kowalik U, Hovinga KE, Geber A, et al. Glioblastoma stem-like cells give rise to tumour endothelium. Nature 2010;468:829-833.
25. Ho DW, Yang ZF, Yi K, Lam CT, Ng MN, Yu WC, et al. Gene expression profiling of liver cancer stem cells by RNA-sequencing. PLoS One 2012;7:e37159.

Hypervascular Hepatocellular Carcinoma: Correlation between Biologic Features and Signal Intensity on Gadoxetic Acid–enhanced MR Images

Azusa Kitao, MD
Osamu Matsui, MD
Norihide Yoneda, MD
Kazuto Kozaka, MD
Satoshi Kobayashi, MD
Wataru Koda, MD
Toshifumi Gabata, MD
Tatsuya Yamashita, MD
Shuichi Kaneko, MD
Yasuni Nakanuma, MD
Ryuichi Kita, MD
Shigeki Arii, MD

Purpose: To analyze the correlation among biologic features, tumor marker production, and signal intensity at gadoxetic acid–enhanced MR imaging in hepatocellular carcinomas (HCCs).

Materials and Methods: Institutional ethics committee approval and informed consent were obtained for this retrospective study. From April 2008 to September 2011, 180 surgically resected HCCs in 180 patients (age, 65.0 years ± 10.3 [range, 34–83 years]; 138 men, 42 women) were classified as either hypointense (n = 158) or hyperintense (n = 22) compared with the signal intensity of the background liver on hepatobiliary phase gadoxetic acid–enhanced MR images. Pathologic features were analyzed and α fetoprotein (AFP) and protein induced by vitamin K absence or antagonist-II (PIVKA-II) production were compared by means of serum analysis and immunohistochemical staining. Recurrence and survival rates were also evaluated. The Mann-Whitney and Pearson correlation tests were used for statistical analysis.

Results: The grade of differentiation was higher (P = .028) and portal vein invasion was less frequent in hyperintense HCCs (13.6%) than in hypointense HCCs (36.7%) (P = .039). The serum levels of AFP, *Lens culinaris* agglutinin reactive fraction of AFP, and PIVKA-II were lower in hyperintense than in hypointense HCCs (P = .003, .004, and .026, respectively). Immunohistochemical AFP and PIVKA-II expression were lower in hyperintense than in hypointense HCCs (both $P < .001$). The recurrence rate was lower in hyperintense than in hypointense HCCs (P = .039).

Conclusion: The results suggest that hyperintense HCCs on gadoxetic acid–enhanced MR images are less aggressive than hypointense HCCs.

Supplemental material: *http://radiology.rsna.org/lookup/suppl/doi:10.1148/radiol.12120226/-/DC1*

[1] From the Departments of Radiology (A.K., O.M., N.Y., K.K., S. Kobayashi, W.K., T.G.), Gastroenterology (T.Y., S. Kaneko), and Human Pathology (Y.N.), Kanazawa University Graduate School of Medical Science, 13-1 Takaramachi, Kanazawa 920-8640, Japan; Department of Gastroenterology, Osaka Red Cross Hospital, Osaka, Japan (R.K.); and Department of Hepatobiliary-Pancreatic Surgery, Tokyo Medical and Dental University, Tokyo, Japan (S.A.). Received February 9, 2012; revision requested March 27; revision received April 24; accepted May 17; final version accepted June 29. Supported in part by a Grant-in-Aid for Scientific Research (21591549) from the Ministry of Education, Culture, Sports, Science and Technology; and by Health and Labor Sciences Research Grants for "Development of novel molecular markers and imaging modalities for earlier diagnosis of hepatocellular carcinoma." **Address correspondence to** A.K. (e-mail: *kitaoa@staff.kanazawa-u.ac.jp*).

Hepatocellular carcinoma (HCC) is the most frequent primary malignant hepatic tumor and the third most common cause of cancer death worldwide (1). The accurate detection and characterization of HCC are critical issues in clinical practice for improving the prognosis of patients with HCC.

Gadoxetic acid–enhanced MR imaging is a new imaging modality with high accuracy for diagnosing HCCs (2–4). On images obtained during the hepatobiliary phase of gadoxetic acid–enhanced MR imaging, HCCs commonly show hypointensity when compared with the background liver. However, approximately 6%–15% of hypervascular HCCs demonstrate iso- or hyperintensity, which is uncommon among hepatic malignant tumors (5–8). This hyperintensity was previously shown to be due to overexpression of organic anion transporting polypeptide 8 (OATP8, synonymous with OATP1B3), which might be the uptake transporter of gadoxetic acid in HCCs (5,6). In the normal liver, OATP8 is expressed on the sinusoidal side of the hepatocyte membrane and takes up many intrinsic and extrinsic organic anions from blood into hepatocytes.

On the other hand, Jung et al (9) showed that OATP8 was up-regulated by hepatocyte nuclear factor 1α. These hepatocyte nuclear factors are indispensable transcription factors that relate to primitive embryonal differentiation of hepatocytes and to hepatocarcinogenesis. We suspected that these atypical hypervascular HCCs that show hyperintensity on hepatobiliary phase images (hyperintense HCC) might reflect a distinct subtype of HCC with a particular molecular background and biologic features.

The main tumor marker of HCCs is α-fetoprotein (AFP), especially the *Lens culinaris* agglutinin reactive fraction (L-3). Similarly, the protein induced by vitamin K absence or antagonist-II (PIVKA-II) is a clinically important serum tumor marker. PIVKA-II is an incomplete coagulation factor prothrombin II whose production is related to the absence of vitamin K or the presence of the antagonist of vitamin K, which is the cofactor of γ carboxylase that converts precursor into prothrombin (10). Serum levels of both AFP and PIVKA-II correlate with the histologic degree of malignancy and the prognosis in HCC (11). In addition, there are reports (12,13) showing that AFP expression in HCCs is regulated by several enhancers and suppressors, including the hepatocyte nuclear factor family. Although the molecular basis of PIVKA-II production is not well explained, we speculated that there might be a correlation of the tumor marker production and signal intensity (SI) on hepatobiliary phase images, which would reflect distinct genomic and proteomic expression of HCC.

The purpose of this study was to analyze the correlation among the pathologic and biologic features, tumor marker production, with SI on hepatobiliary phase gadoxetic acid–enhanced MR images of HCCs.

Advances in Knowledge

- Hypervascular hepatocellular carcinomas (HCCs) that hyperintensity relative to the surrounding liver on hepatobiliary phase gadoxetic acid–enhanced MR images demonstrate a significantly higher grade of differentiation ($P = .028$) and rarer portal vein invasion ($P = .039$) than those of hypointense HCCs.
- Hyperintense HCCs on hepatobiliary phase gadoxetic acid–enhanced MR images show significantly lower serum level of α fetoprotein, *Lens culinaris* agglutinin reactive fraction of α fetoprotein, and protein induced by Vitamin K absence or antagonist-II than hypointense HCCs ($P = .003$, $P = .004$, and $P = .026$, respectively).
- Hyperintense HCCs on hepatobiliary phase gadoxetic acid–enhanced MR images similarly show significantly weaker expression of α fetoprotein and protein induced by Vitamin K absence or antagonist-II at immunohistochemical evaluation than did hypointense HCCs (both $P < .001$).
- Hyperintense HCCs on gadoxetic acid–enhanced MR images show a significantly lower recurrence rate than do hypointense HCCs ($P = .039$).

Implication for Patient Care

- Hypervascular HCCs that show hyperintensity on hepatobiliary phase gadoxetic acid–enhanced MR images have biologically less aggressive features than do those that show hypointensity.

Materials and Methods

Patients

This retrospective study received the approval of the institutional ethics committee, and informed consent for using the MR images and resected specimens was obtained from all patients. There were 207 consecutive patients who had 233 HCCs that were surgically resected

Published online
10.1148/radiol.12120226 **Content codes:** GI MR

Radiology 2012; 265:780–789

Abbreviations:
AFP = α-fetoprotein
HCC = hepatocellular carcinoma
L-3 = *Lens culinaris* agglutinin reactive fraction
mAU = milli–arbitrary unit
OATP = organic anion transporting polypeptide
PIVKA-II = protein induced by vitamin K absence or antagonist-II
SI = signal intensity
TR = repetition time

Author contributions:
Guarantors of integrity of entire study, A.K., O.M., K.K., S. Kobayashi, T.G., S. Kaneko, Y.N., S.A.; study concepts/study design or data acquisition or data analysis/interpretation, all authors; manuscript drafting or manuscript revision for important intellectual content, all authors; approval of final version of submitted manuscript, all authors; literature research, A.K., O.M., N.Y., K.K., S. Kobayashi, S. Kaneko, Y.N., S.A.; clinical studies, A.K., O.M., K.K., S. Kobayashi, W.K., T.G., T.Y., S. Kaneko, R.K., S.A.; experimental studies, A.K., N.Y., Y.N., S.A.; statistical analysis, A.K.; and manuscript editing, A.K., O.M., S. Kobayashi, T.G., S. Kaneko, S.A.

Conflicts of interest are listed at the end of this article.

at our institution and six affiliated institutions from April 2008 to September 2011. Patients were excluded if they had more than one HCC (12 patients with 31 nodules), if they had previous treatment (three patients with 10 nodules), if they did not have MR imaging (nine patients with nine nodules) or if their lesions were hypovascular in the arterial phase (three patients with three nodules) (Fig E1 [online]). Average age was 65.0 years ± 10.3 (range, 34–83) (age of men 64.5 years ± 10.5 [range, 34–83 years]; women, 67.4 years ± 9.5 [43–83 years]). Ratio of men to women was 138 (76.7%) to 42 (23.3%). The background liver was normal in 28 patients, whereas 70 patients had chronic hepatitis and 82 had cirrhosis. The origin of liver disease was viral hepatitis type B in 41 patients, type C in 85, types B and C in two, alcoholism in nine, and other origins in 43. Hepatic function was classified as Child-Pugh class A in 169 patients and class B in 11. Average tumor size was 33.8 mm ± 23.4 (range, 7–160 mm).

Gadoxetic Acid–enhanced MR Imaging

Gadoxetic acid–enhanced MR imaging was performed 52.8 days ± 25.3 [range, 3–95 days] before surgical resection for the characterization and pretreatment staging of HCC. MR images were obtained on several MR systems: Signa HDx 1.5 T and 3 T (GE Medical Systems, Milwaukee, Wis), Intera Achieva 1.5 T (Philips Medical Systems, Best, Netherlands), Symphony 1.5 T (Siemens, Erlangen, Germany) and Magnetom Vision 1.5 T (Siemens). MR imaging was performed with fat-suppressed two-dimensional or three-dimensional gradient-echo T1-weighted sequences (repetition time, 3.2–4.0 msec; echo time, 1.6–2.3 msec; flip angle, 10–15 degrees; field of view, 33–42 cm; matrix, 128–192 interpolated to 256–512; section thickness, 4.0–8.0 mm). For dynamic study, a dose of 0.1 mL per kilogram of 0.25 mmol/mL of gadoxetic acid (Primovist, Bayer Schering Pharma, Berlin) was injected intravenously at a flow rate of 1–2.0 mL per second, followed by a 20–40 mL saline flush. To obtain the optimal arterial dominant phase, the following methods were used. In the bolus tracking method, arterial phase timing was determined as the peak time of the abdominal aorta plus 7–15 seconds. In the test injection method (1.5 mL of Primovist + 8 mL saline flush), arterial-phase timing was determined as the peak time of the abdominal aorta plus 10 seconds minus half of imaging time. Portal phase and equilibrium phase images were obtained at 60–90 seconds and 120–180 seconds after injection, respectively. The hepatobiliary phase images were obtained 15–20 minutes after the injection.

Analysis of SI on Gadoxetic Acid–enhanced MR Images

Image analysis was performed by two abdominal imaging radiologists (A.K. and O.M., with 10 and 40 years of experience, respectively) without information on clinical and pathologic results. The SI of the tumor and surrounding background liver was individually measured and then averaged by placing regions of interest during the hepatobiliary phase. The region of interest of the tumor was determined as the maximum oval or round area at the level of the largest diameter of the tumor, avoiding degeneration area and artifact. The average size of the region of interest was 923.6 mm^2 ± 1418.3 (range, 61–6167 mm^2). The average intensity of the entire region of interest was used for analysis. A region of interest of the same size as the tumors was placed on the adjacent liver parenchyma, avoiding the large vessels.

Hypointense HCC was defined as showing lower SI than that of the surrounding liver (tumor SI/background SI < 1.0) (Fig 1a), and hyperintense HCC as showing equal or higher SI (tumor SI/background SI ≥ 1.0) (Fig 2a).

The Enhancement Ratio in the Hepatobiliary Phase

To evaluate the uptake level of gadoxetic acid, we calculated the enhancement ratio of HCCs in the hepatobiliary phase. We could not consistently assess all patients because they were examined with various MR systems and by using somewhat different parameters. As a result, we focused on only 79 HCCs studied at our institution because they were imaged by a variable flip angle method for measuring T1 value. MR images were obtained with either a 1.5-T or 3-T MR system (Signa HDx; GE Medical Systems, Milwaukee, Wis). MR imaging was performed with fat-suppressed three-dimentional spoiled gradient-echo in the steady state T1-weighted sequences (liver acquisition with volume acceleration; generalized encoding matrix; repetition time, 3.2–4.0 msec; echo time, 1.6 msec; flip angle, 6–15 degrees; field of view, 42 × 42 cm; matrix, 192 × 320, interpolated to 512 × 512; section thickness, 4.2 mm; overlap, 2.1 mm). The unenhanced phase was imaged with two different flip angles to calculate the static T1 value. The hepatobiliary phase images were obtained 20 minutes after the injection. The static T1 value before enhancement ($T1_{pre}$) was calculated as follows:

$$\exp(-TR/T1_{pre}) = (SI_A \sin\beta - S_B \sin\alpha)/(SI_A \sin\beta \cos\alpha - SI_B \sin\alpha \cos\beta)$$

where TR is repetition time and SI_A and SI_B represent the signal intensity in flip angle α and β, respectively. The enhanced images were obtained with the same parameters by using flip angle α. Then the T1 value after enhancement ($T1_{post}$) was calculated as follows:

$$\exp(-TR/T1_{post}) = \{SI_{pre}[1-\exp(-TR/T1_{pre})\cos\alpha] + SI_{post}[\exp(-TR/T1_{pre})-1]\} / \{SI_{pre}[1-\exp(-TR/T1_{pre})\cos\alpha] + SI_{post}[\exp(-TR/T1_{pre})-1]\cos\alpha\}$$

The enhancement ratio was shown as (8)

$$(1/T1_{post} - 1/T1_{pre})/(1/T1_{pre})$$

Histologic Diagnosis

Hematoxylin and eosin staining was carried out in tissue sections of all 180

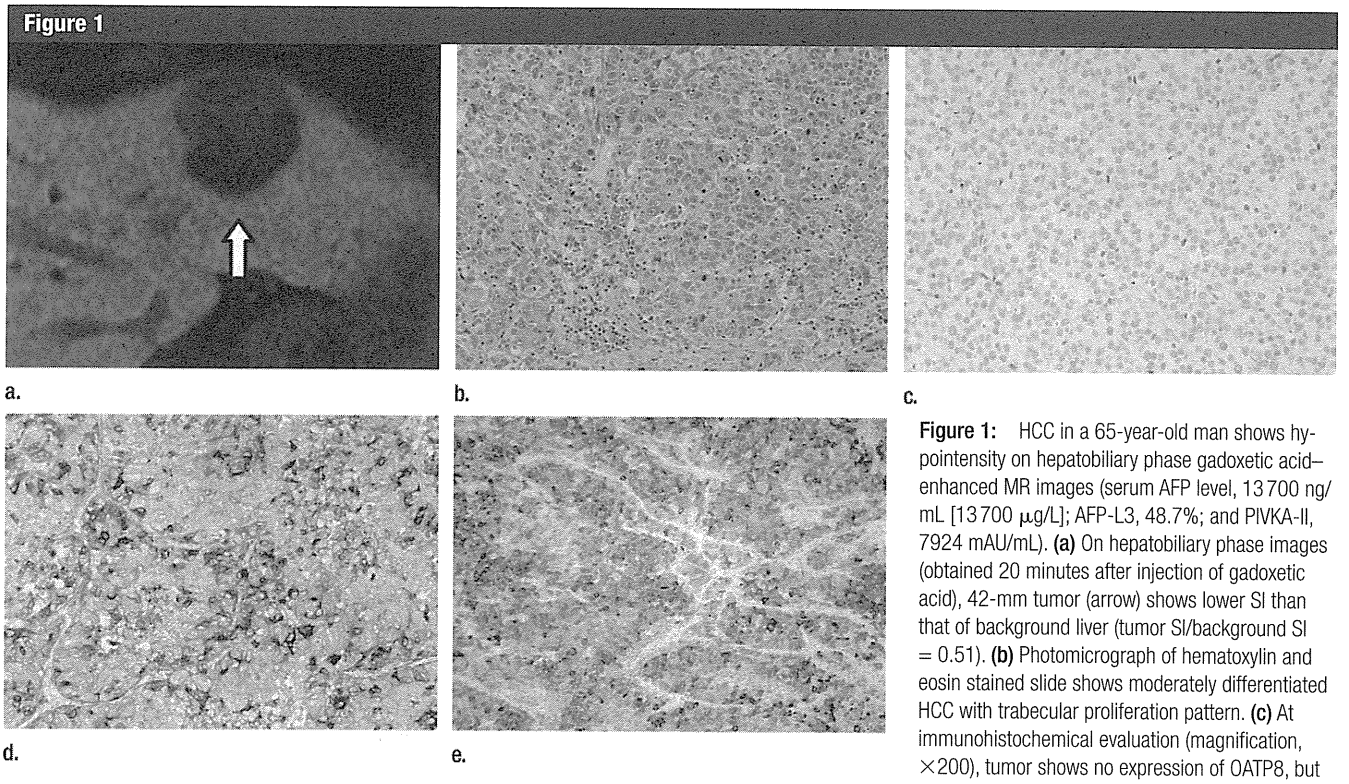

Figure 1: HCC in a 65-year-old man shows hypointensity on hepatobiliary phase gadoxetic acid–enhanced MR images (serum AFP level, 13 700 ng/mL [13 700 μg/L]; AFP-L3, 48.7%; and PIVKA-II, 7924 mAU/mL). **(a)** On hepatobiliary phase images (obtained 20 minutes after injection of gadoxetic acid), 42-mm tumor (arrow) shows lower SI than that of background liver (tumor SI/background SI = 0.51). **(b)** Photomicrograph of hematoxylin and eosin stained slide shows moderately differentiated HCC with trabecular proliferation pattern. **(c)** At immunohistochemical evaluation (magnification, ×200), tumor shows no expression of OATP8, but **(d)** intense expression of both AFP (brown color) and **(e)** PIVKA-II (brown color).

liver specimens. HCCs were diagnosed by consensus of two liver pathologists (S.K and Y.N. with 10 and 38 years of experience, respectively), according to the classification proposed by the International Working Party (14) and the World Health Organization classification (15). We compared hypointense HCCs and hyperintense HCCs with regard to histologic features such as macroscopic growth patterns (indistinct margin, simple nodular, extranodular growth, and multinodular patterns) (16), differentiation grade (well, moderately, and poorly differentiated), proliferation pattern (trabecular, pseudoglandular, scirrhous, and compact pattern), fibrous capsule invasion, portal vein invasion and hepatic vein invasion.

Measuring Serum Levels of AFP and PIVKA-II

Preoperative patient serum levels were obtained 10.2 days ± 7.3 (range, 0–35 days) before or after MR imaging. Serum AFP levels were measured by using chemiluminescent enzyme immunoassay (Lumipulse presto; Fujirebio, Tokyo, Japan). Serum AFP-L3 levels were measured by means of liquid-phase binding assay-electrokinetic analyte transport assay (LBA AFP-L3; Wako Pure Chemical Industries, Osaka, Japan), and were expressed as the ratio of AFP-L3 to total AFP percentage. Serum PIVKA-II levels were measured by electrochemiluminescence immunoassay (Picolumi PIVKA-II; Eidia, Tokyo, Japan) and were expressed in milli-arbitrary units (mAUs).

Immunohistochemical Analysis of AFP, PIVKA-II, and OATP8

Immunostaining was performed for all HCC specimens by using the primary antibodies human AFP (rabbit polyclonal; DAKO, Glostrup, Denmark), human PIVKA-II (MU-3 mouse monoclonal; Eidia, Tokyo, Japan) and human OATP8 (mouse monoclonal NB100-74482; Novus Biologicals, Littleton, Colo).

Two abdominal imaging radiologists (N.Y. and A.K., with 9 and 10 years of experience, respectively, in radiology and pathologic research) independently and blindly evaluated the intensity of the AFP and PIVKA-II expression on tumor cytoplasm as follows: grade 0, no expression; grade 1, weak expression; grade 2, moderate expression; and grade 3, strong expression. Similarly, they semiquantitatively evaluated the intensity of OATP8 expression on tumor cellular membranes compared with the background hepatocytes as follows: grade 0, no expression; grade 1, decreased expression; grade 2, equivalent expression; and grade 3, increased expression. We analyzed the average grades of the two investigators.

Then, we compared hypointense and hyperintense HCCs for clinical and histologic features and AFP/PIVKA-II expression (serum level and immunohistochemical analysis). To examine whether the AFP and PIVKA level simply correlates with the differentiation grade of HCCs, we performed the same analysis excluding 42 poorly differentiated HCCs. We analyzed the correlation

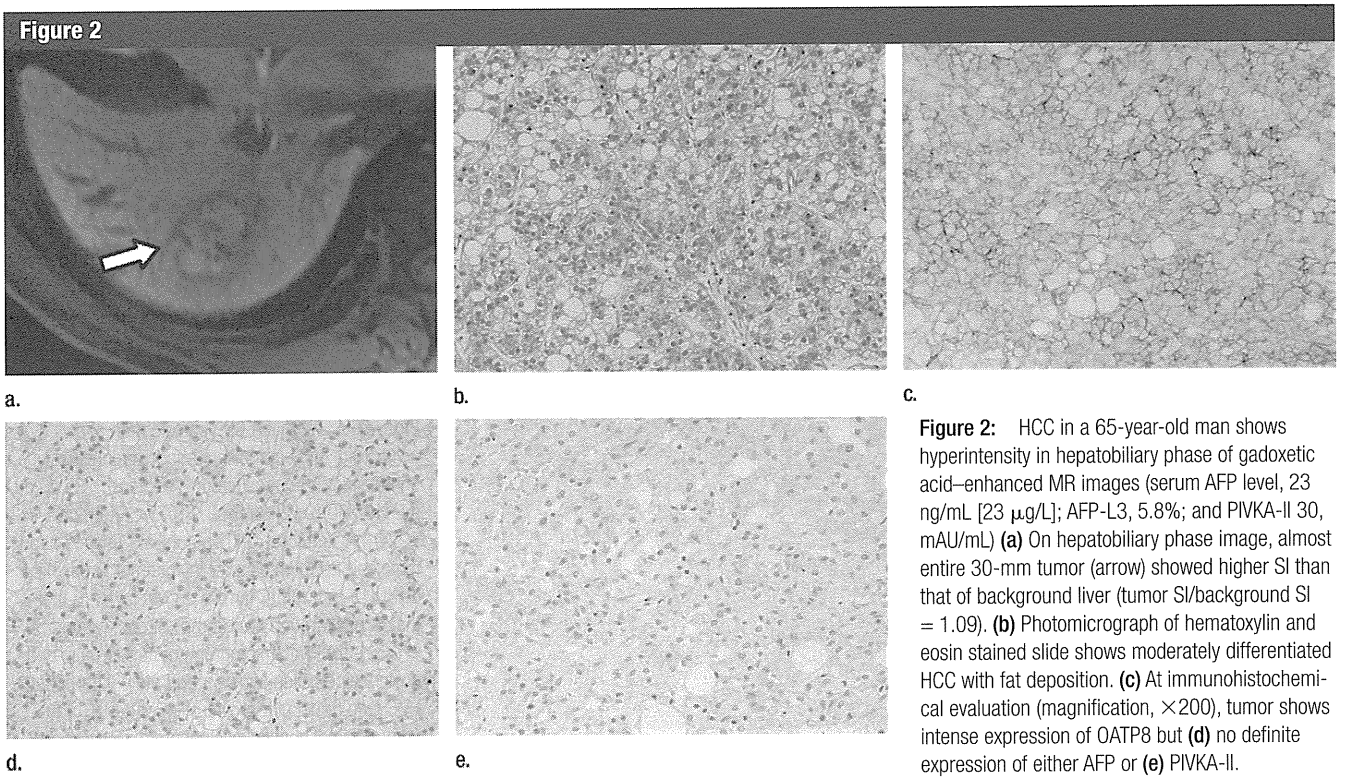

Figure 2: HCC in a 65-year-old man shows hyperintensity in hepatobiliary phase of gadoxetic acid–enhanced MR images (serum AFP level, 23 ng/mL [23 μg/L]; AFP-L3, 5.8%; and PIVKA-II 30, mAU/mL) **(a)** On hepatobiliary phase image, almost entire 30-mm tumor (arrow) showed higher SI than that of background liver (tumor SI/background SI = 1.09). **(b)** Photomicrograph of hematoxylin and eosin stained slide shows moderately differentiated HCC with fat deposition. **(c)** At immunohistochemical evaluation (magnification, ×200), tumor shows intense expression of OATP8 but **(d)** no definite expression of either AFP or **(e)** PIVKA-II.

among the immunohistochemical AFP, PIVKA-II, and OATP8 expression. We also analyzed the correlation among enhancement ratio and serum levels and immunohistochemical AFP and PIVKA-II expression for 79 HCCs.

Recurrence and Survival Rates in Patients with HCC

We compared the two groups for recurrence (including all local recurrence and intrahepatic and extrahepatic metastasis) and survival duration from the operation day. The follow-up length was 727 days ± 365 (range, 22–1293 days). When intrahepatic hypervascular HCCs or obvious extrahepatic metastasis appeared on follow-up dynamic computed tomography or gadoxetic acid–enhanced MR imaging, we considered it to be recurrence.

Statistical Analyses

Statistical significance was evaluated with GraphPad Prism5 (GraphPad Software, San Diego, Calif) and Excel Statistics 2010 (Social Survey Research Information, Tokyo, Japan). We used the Fisher test for the analysis of the clinical and histologic features; Mann-Whitney test for the comparison of serum and immunohistochemical tumor marker levels; Pearson correlation test for the correlations among AFP, PIVKA-II, OATP8 expression and enhancement ratio; and κ test for the evaluation of interobserver variation in the analysis of immunohistochemistry. The κ test score (the level of agreement) was defined as follows: 0.0–0.40, poor; 0.41–0.60, moderate; 0.61–0.80, good to fair; and 0.81–1.0, excellent. Kaplan-Meier analysis with Log-rank test, logistic regression, and Cox regression were performed for the evaluation of clinical outcome and recurrence. A P value less than 0.05 was considered to indicate a statistically significant difference.

Results

Clinical Features of the Two Types of HCC

One hundred and fifty-eight nodules were classified as hypointense HCCs (average tumor SI/background SI, 0.46 ± 0.11; range, 0.24–0.67) and the remaining 22 nodules were classified as hyperintense HCC (average tumor SI/background SI, 1.19 ± 0.22; range, 1.06–1.86). No significant differences were observed in clinical features such as sex, background liver, liver function, or tumor size between the patients with hypointense HCC and hyperintense HCC, but there was a significant difference for age (Table 1). The patients with hyperintense HCCs were significantly older than those with hypointense HCCs (P = .04).

Pathologic Features of the Two Types of HCC

None of the differences noted in the macroscopic growth patterns between the hypointense and hyperintense HCCs were significant (P = .77) (Fig E2a [online]). The hyperintense HCCs showed significantly higher differentiation grade than the hypointense HCCs (P = .028) (Fig E2b [online]). Pseudoglandular pattern was more frequently seen in hyperintense HCCs than in hypointense HCCs (Fig E2c [online]). There was a significant difference in the proliferation

Table 1

Clinical Features of Patients

Clinical Features	Hypointense HCCs	Hyperintense HCCs	*P* Value
No. of tumors	158	22	
Resected tumor size (mm)	33.2 ± 22.9 (7–160)*	37.7 ± 18.9 (10–105)*	.38
Age (y)	64.6 ± 10.3 (34–83)*	69.5 ± 7.8 (52–81)*	.04
Sex			.30
Men	119	3	
Women	39	19	
Background liver tissue			.23
Normal liver	23	5	
Chronic hepatitis	65	5	
Liver cirrhosis	70	12	
Origin of liver disease			.10
Hepatitis B	38	3	
Hepatitis C	74	11	
Hepatitis B and C	2	0	
Alcoholism	6	3	
Other	38	5	
Child Pugh classification			.63
A	149	20	
B	9	2	

Note.—Unless otherwise indicated, data are number of patients.

* Data are means ± standard deviations, with ranges in parentheses.

pattern between the hypointense and hyperintense HCCs ($P < .001$). The hypointense HCCs showed higher positive rates for fibrous capsule invasion and hepatic vein invasion, although the differences did not reach statistical significance ($P = .81$ and .21, respectively). The hyperintense HCCs showed a significantly lower rate of portal vein invasion than that of hypointense HCCs ($P = .039$) (Fig E2e [online]).

Serum Levels of AFP, AFP-L3 Fraction, and PIVKA-II

The serum levels of tumor markers AFP, AFP-L3, and PIVKA-II were significantly lower in the patients with hyperintense HCCs than in those with hypointense HCCs ($P = .003$, .004, and .026) (Figs 3, E3 [online]). To examine whether the AFP and PIVKA levels correlated with the differentiation grade of the HCCs, we performed the same analysis, excluding 42 poorly differentiated HCCs (Fig E4 [online]). Despite excluding poorly differentiated HCCs, the serum levels of these markers were also lower in the patients with hyperintense HCCs than in those with hypointense HCCs ($P = .005$, .019, and .08).

Immunohistochemistry of AFP and PIVKA-II in HCCs

In the semiquantitative analyses of immunohistochemical OATP8, AFP, and PIVKA-II, interobserver agreement of the two readers was good to excellent ($\kappa = 0.82$, 0.78, and 0.81, respectively). In immunohistochemical analysis, OATP8 expression was significantly decreased in hypointense HCCs compared with that in hyperintense HCCs ($P < .001$) (Fig 4a). The AFP expression was significantly higher in hypointense HCCs than that in hyperintense HCCs ($P < .001$) (Fig 4b). There was a significant negative correlation between AFP expression and OATP8 expression ($P = .002$, $R = -0.22$) (Fig E5c [online]). The immunohistochemical PIVKA-II expression was also significantly higher in hypointense HCCs than that in hyperintense HCCs ($P < .001$) (Fig 4c). There was a significant negative correlation between PIVKA-II expression and OATP8 expression ($P < .001$, $R = -0.38$) (Fig E5e [online]). We also performed the same immunohistochemical analysis excluding poorly differentiated HCCs (Fig E6 [online]). The expression of OATP8 was significantly lower, but expression of AFP and PIVKA-II was significantly higher in hypointense HCCs than those in hyperintense HCCs (both $P < .001$). There was still a significant negative correlation between AFP and OATP8 expression ($P = .0017$, $R = -0.27$) and between PIVKA-II and OATP8 expression ($P < .001$, $R = -0.46$).

Relative Enhancement Ratio on Hepatobiliary Phase and AFP or PIVKA-II Production

We analyzed the correlation between relative enhancement ratio and tumor marker expression for 79 HCCs (69 hypointense and 10 hyperintense HCCs). Significant negative correlations were noted among the enhancement ratio and serum AFP ($P = .023$, $R = -0.25$), serum AFP-L3 ($P < .001$, $R = -0.49$) and serum PIVKA-II level ($P = .018$, $R = -0.26$) (Fig E7a, E7b [online]). At immunohistochemical analysis, we also confirmed significant negative correlations among the enhancement ratio and AFP expression ($P = .007$, $R = -0.30$) and PIVKA-II expression ($P = .009$, $R = -0.29$) (Fig E7d, E7e [online]).

Analysis of Prognosis in Patients with HCC

The patients with hyperintense HCCs showed a significantly lower recurrence rate than those with hypointense HCCs ($P = .039$). The patients with hyperintense HCCs tended to show longer survival than those with hypointense HCCs, although without significant difference ($P = .07$) (Fig 5). Clinical features such as age and tumor size did not affect the recurrence and survival curves (Table E1 [online]). The summary of results is shown in Table 2.

Discussion

In our study, hyperintense HCCs in the hepatobiliary phase showed sig

Figure 3

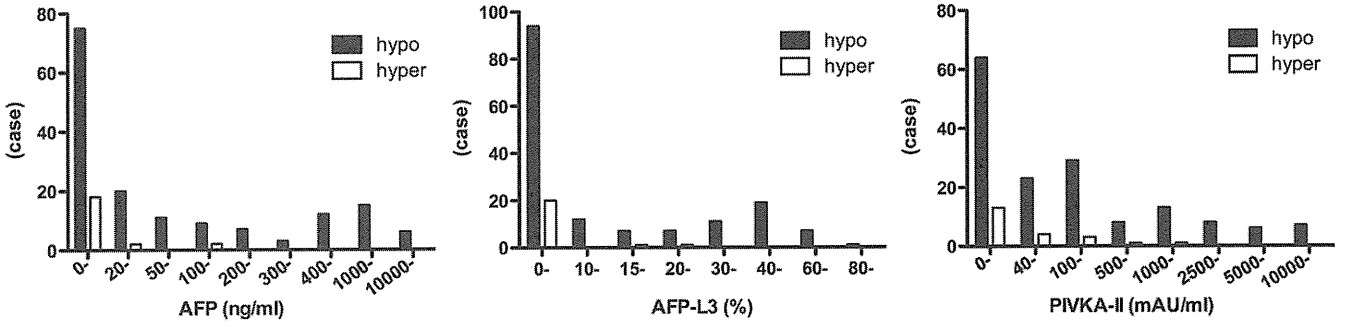

Figure 3: Graphs show serum levels of AFP, AFP-L3, and PIVKA-II. **(a)** Serum level of AFP was in normal range (<20 ng/mL [<20 μg/L]) in 18 of 22 patients (82%) with hyperintense HCCs and in 75 of 158 (47%) of patients with hypointense HCCs. Average serum AFP value was 1202.7 ng/mL ± 4369.9 [1202.7 μg/L ± 4369.9] in patients with hypointense HCCs and 17.9 ng/mL ± 29.0 [17.9 μg/L ± 29.0] in patients with hyperintense HCC, ($P = .003$). **(b)** Serum level of AFP-L3 was in normal range (<10%) in 20 of 22 patients (91%) with hyperintense HCCs, and 94 of 158 (59%) patients with hypointense HCCs. Average serum AFP-L3 fraction value was significantly lower in patients with hyperintense HCC (3.8% ± 7.5) than in those with hypointense HCC (15.9% ± 21.2) ($P = .004$). **(c)** Serum level of PIVKA-II was in normal range (<40 mAU/mL) in 13 of 22 (59%) patients with hyperintense HCCs, and 64 of 158 (40%) patients with hypointense HCCs. The serum level of PIVKA-II was also lower in patients with hyperintense HCCs (190.6 mAU/mL ± 468.6) than those with hypointense HCCs (1697.9 mAU/mL ± 6232.0) ($P = .026$).

Figure 4

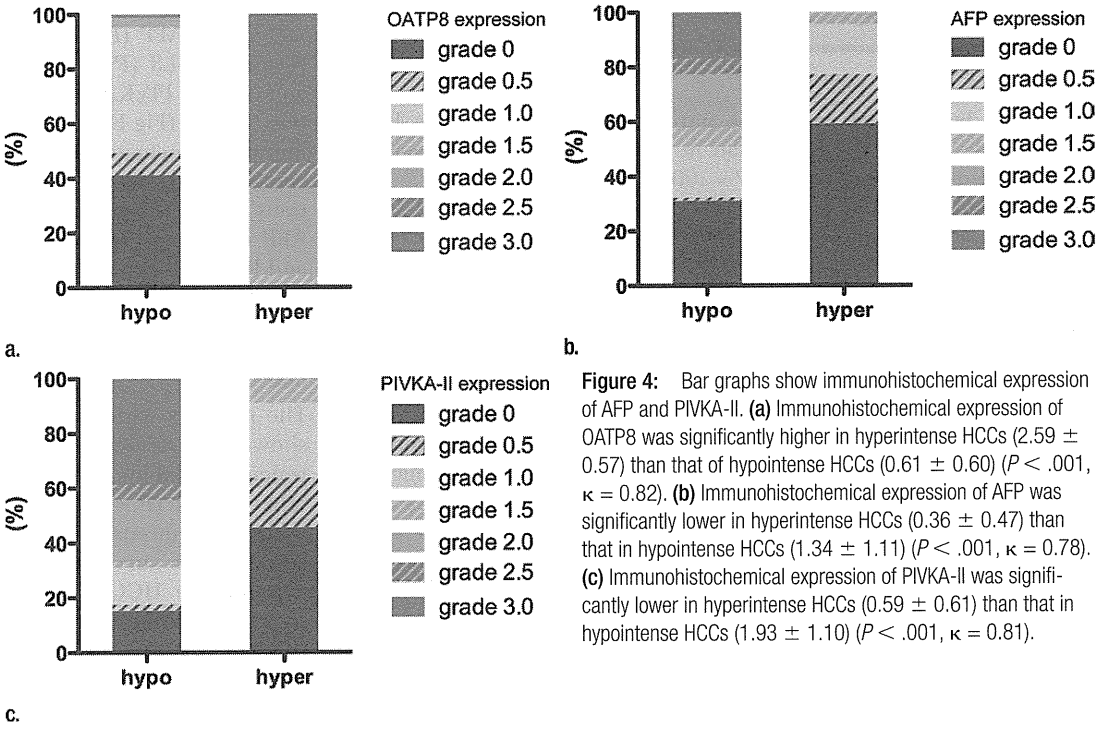

Figure 4: Bar graphs show immunohistochemical expression of AFP and PIVKA-II. **(a)** Immunohistochemical expression of OATP8 was significantly higher in hyperintense HCCs (2.59 ± 0.57) than that of hypointense HCCs (0.61 ± 0.60) ($P < .001$, $\kappa = 0.82$). **(b)** Immunohistochemical expression of AFP was significantly lower in hyperintense HCCs (0.36 ± 0.47) than that in hypointense HCCs (1.34 ± 1.11) ($P < .001$, $\kappa = 0.78$). **(c)** Immunohistochemical expression of PIVKA-II was significantly lower in hyperintense HCCs (0.59 ± 0.61) than that in hypointense HCCs (1.93 ± 1.10) ($P < .001$, $\kappa = 0.81$).

nificantly higher differentiation grades with lower frequency of portal vein invasion than did the hypointense HCCs. Moreover, hyperintense HCCs showed significantly lower expression of AFP and PIVKA-II than did hypointense HCCs. AFP and PIVKA-II levels correlated with the histologic grade of malignancy and poor prognosis (11); however, we demonstrated that the difference in tumor marker production between hypointense HCCs and hyperintense HCCs did not depend on the differentiation grade when poorly differentiated HCCs were excluded

Figure 5

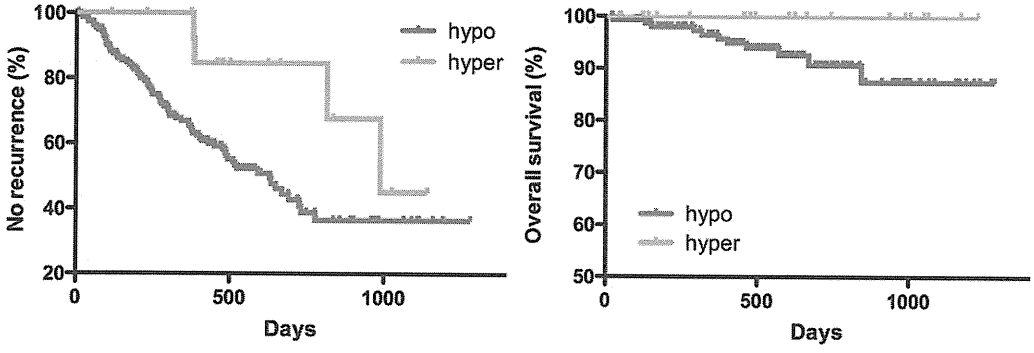

Figure 5: Charts show prognosis of patients with HCC. **(a)** Patients with hyperintense HCCs showed significantly lower recurrence rate (6 of 22, 27.2%) than did those with hypointense HCCs (83 of 158, 52.5%) ($P = .039$). **(b)** Patients with hyperintense HCCs tended to show longer survival (mortality, 0 of 22, 0%) than those with hypointense HCCs (22 of 158, 13.9%). However, there was no significant difference between the two groups ($P = .07$).

Table 2

Summary of Results

Result	Hypointense HCCs ($n = 158$)	Hyperintense HCCs ($n = 22$)	*P* Value
Macro growth pattern			.77
Indistinct margin	6	0	
Simple nodular	102	17	
Extranodular	30	3	
Multinodular	20	2	
Differentiation			.028
Well differentiated	22	4	
Moderately differentiated	94	18	
Poorly differentiated	42	0	
Proliferation pattern			<.001
Trabecular	116	12	
Pseudoglandular	20	10	
Schirrous	9	0	
Compact	13	0	
Fibrous capsule invasion	63 (39.9%)	8 (36.4%)	.810
Portal vein invasion	58 (36.7%)	3 (13.6%)	.039
Hepatic vein invasion	21 (13.3%)	0 (0%)	.210
Serum levels			
AFP (ng/mL)	1202.7 ± 4369.9 (497.4 ± 1899.1*)	17.9 ± 29.0	.003 (.005*)
AFP-L3 (%)	15.9 ± 21.2 (14.5 ± 21.0*)	3.8 ± 7.5	.004 (.019*)
PIVKA-II (mAU/mL)	1697.9 ± 6232.0 (1497.6 ± 7067.9*)	190.6 ± 468.6	.026 (.08*)
Immunohistochemical analysis			
OATP8	0.61 ± 0.60 (0.67 ± 0.63*)	2.59 ± 0.57	<.001 (<.001*)
AFP	1.34 ± 1.11 (1.34 ± 1.10*)	0.36 ± 0.47	<.001 (<.001*)
PIVKA-II	1.93 ± 1.10 (1.87 ± 1.08*)	0.59 ± 0.61	<.001 (<.001*)
Recurrence rate	83 (52.5%)	6 (27.2%)	.039
Survival rate	22 (86.1%)	22 (100%)	.070

* Excluding poorly differentiated HCCs ($n = 42$).

from the analysis. We suspect that the molecular regulatory mechanism of OATP8 expression may have some common channels with those of AFP or PIVKA-II expression.

In addition, hyperintense HCCs on hepatobiliary phase images showed a significantly lower recurrence rate than did hypointense HCCs. The patients with hyperintense HCCs showed longer survival than those with hypointense HCCs, but the difference was not statistically significant. In our study, the follow-up period averaged 727 days, which might not have been sufficient to demonstrate a significant difference.

Several prior reports have suggested that transcription factor hepatocyte nuclear factors control both OATP8 and AFP expression (9,12,13,17). Therefore, we speculated that some correlation between OATP8 and AFP expression through the hepatocyte nuclear factor family might exist. The regulatory mechanism of PIVKA-II and the correlation with OATP8 expression in HCC have not yet been determined. The transcription of the OATP8 gene is also regulated by the nuclear factor (steroid and xenobiotics receptor or pregnane xenobiotics receptor) (18). Vitamin K can be the ligand of these receptors, and it regulates the transcription of target genes (19). If vitamin

K decreases in HCC, the PIVKA-II production increases (20). We suspected that the transcription of OATP8 might change in accordance with the decrease of ligands to these receptors. As a result, we expected that PIVKA-II expression and OATP8 expression might be correlated.

However, there were many patients that showed low AFP and PIVKA-II expression in hypointense HCCs. We attribute this to the fact that OATP8, AFP, and PIVKA-II have several direct and indirect regulatory mechanisms other than the hepatocyte nuclear factor route (21). Further investigation is needed to clarify the real underlying molecular biology of these correlations.

The molecular classification of subtypes of HCCs is now being investigated by several groups (22). Yamashita et al (23,24) reported on HCC subtypes that were classified on the basis of expression of AFP and epithelial cell adhesion molecule, a stem cell marker. According to their reports, AFP-positive and epithelial cell adhesion molecule–positive HCCs showed stem and progenitor cell features with invasive character and poor prognosis compared with AFP-negative and epithelial cell adhesion molecule–negative HCCs that demonstrated mature hepatocyte-like features with a relatively good prognosis. These features of AFP-negative and epithelial cell adhesion molecule–negative HCCs resembled those of hyperintense HCCs, and we surmised that the origin of hyperintense HCC may be mature hepatocyte-like cells rather than stem or progenitor cells. We think that hyperintense HCCs may have some specific molecular or genetic profiles. Further molecular and genetic analyses are needed to clarify the exact molecular biologic basis for this possible subtype of HCCs.

Our study had limitations. First, the total number of hyperintense HCCs examined was small because such tumors are relatively rare (8). Second, we only assessed HCC lesions that were hypervascular in the arterial phase, and therefore our results cannot be applied to a general screening population with benign disease, hypovascular HCC on arterial-phase images, or other malignancies. Third, there was a variability of the imaging parameters, such as strength of magnetic field, section thickness, and on imaging timing, because this was multicenter study.

In conclusion, hyperintense HCCs on hepatobiliary phase images showed significantly higher differentiation grades, less frequent portal vein invasion, and lower recurrence rates than did hypointense HCCs. Moreover, hyperintense HCCs showed significantly lower expression of AFP and PIVKA-II than did hypointense HCCs. Hyperintense HCCs on hepatobiliary phase gadoxetic acid–enhanced MR images may be a particular form of hypervascular HCC with biologically less aggressive features than those of hypointense HCCs.

Acknowledgments: We deeply appreciate Dr. Taro Yamashita (Department of Gastroenterology, Kanazawa University Graduate School of Medical Science, Kanazawa, Japan), Dr. Yoh Zen (Institute of Liver Studies, King's College Hospital, London, United Kingdom) and Dr. Seiko Kitamura-Sawada (Division of Pathology, Kanazawa University Hospital, Kanazawa, Japan) for their support to our study.

Disclosures of Conflicts of Interest: A.K. No relevant conflicts of interest to disclose. **O.M.** Financial activities related to the present article: Received a consulting fee or honorarium and fees for participation in review activities from Bayer Japan. Financial activities not related to the present article: none to disclose. Other relationships: none to disclose. **N.Y.** No relevant conflicts of interest to disclose. **K.K.** No relevant conflicts of interest to disclose. **S.Kobayashi.** No relevant conflicts of interest to disclose. **W.K.** No relevant conflicts of interest to disclose. **T.G.** No relevant conflicts of interest to disclose. **T.Y.** No relevant conflicts of interest to disclose. **S.Kaneko.** No relevant conflicts of interest to disclose. **Y.N.** No relevant conflicts of interest to disclose. **R.K.** No relevant conflicts of interest to disclose. **S.A.** No relevant conflicts of interest to disclose.

References

1. Caldwell S, Park SH. The epidemiology of hepatocellular cancer: from the perspectives of public health problem to tumor biology. J Gastroenterol 2009;44(Suppl 19):96–101.
2. Ahn SS, Kim MJ, Lim JS, Hong HS, Chung YE, Choi JY. Added value of gadoxetic acid-enhanced hepatobiliary phase MR imaging in the diagnosis of hepatocellular carcinoma. Radiology 2010;255(2):459–466.
3. Ichikawa T, Saito K, Yoshioka N, et al. Detection and characterization of focal liver lesions: a Japanese phase III, multicenter comparison between gadoxetic acid disodium-enhanced magnetic resonance imaging and contrast-enhanced computed tomography predominantly in patients with hepatocellular carcinoma and chronic liver disease. Invest Radiol 2010;45(3):133–141.
4. Golfieri R, Renzulli M, Lucidi V, Corcioni B, Trevisani F, Bolondi L. Contribution of the hepatobiliary phase of Gd-EOB-DTPA-enhanced MRI to Dynamic MRI in the detection of hypovascular small (≤ 2 cm) HCC in cirrhosis. Eur Radiol 2011;21(6):1233–1242.
5. Kitao A, Zen Y, Matsui O, et al. Hepatocellular carcinoma: signal intensity at gadoxetic acid-enhanced MR Imaging—correlation with molecular transporters and histopathologic features. Radiology 2010;256(3):817–826.
6. Narita M, Hatano E, Arizono S, et al. Expression of OATP1B3 determines uptake of Gd-EOB-DTPA in hepatocellular carcinoma. J Gastroenterol 2009;44(7):793–798.
7. Asayama Y, Tajima T, Nishie A, et al. Uptake of Gd-EOB-DTPA by hepatocellular carcinoma: radiologic-pathologic correlation with special reference to bile production. Eur J Radiol 2011;80(3):e243–e248.
8. Kitao A, Matsui O, Yoneda N, et al. The uptake transporter OATP8 expression decreases during multistep hepatocarcinogenesis: correlation with gadoxetic acid enhanced MR imaging. Eur Radiol 2011;21(10):2056–2066.
9. Jung D, Hagenbuch B, Gresh L, Pontoglio M, Meier PJ, Kullak-Ublick GA. Characterization of the human OATP-C (SLC21A6) gene promoter and regulation of liver-specific OATP genes by hepatocyte nuclear factor 1 alpha. J Biol Chem 2001;276(40):37206–37214.
10. Inagaki Y, Tang W, Xu H, et al. Des-gamma-carboxyprothrombin: clinical effectiveness and biochemical importance. Biosci Trends 2008;2(2):53–60.
11. Miyaaki H, Nakashima O, Kurogi M, Eguchi K, Kojiro M. Lens culinaris agglutinin-reactive alpha-fetoprotein and protein induced by vitamin K absence II are potential indicators of a poor prognosis: a histopathological study of surgically resected hepatocellular carcinoma. J Gastroenterol 2007;42(12):962–968.
12. Nakabayashi H, Koyama Y, Suzuki H, et al. Functional mapping of tissue-specific elements of the human alpha-fetoprotein gene enhancer. Biochem Biophys Res Commun 2004;318(3):773–785.

13. Ishii K, Yoshida Y, Akechi Y, et al. Hepatic differentiation of human bone marrow-derived mesenchymal stem cells by tetracycline-regulated hepatocyte nuclear factor 3beta. Hepatology 2008;48(2):597–606.

14. Hirohashi S, Ishak KG, Kojiro M, et al. Hepatocellular carcinoma. In: Hamilton SR, Aaltonen LA, eds. Pathology and genetics of tumours of the digestive system. Lyon, France: IARC, 2000; 157–172.

15. International Consensus Group for Hepatocellular Neoplasia. Pathologic diagnosis of early hepatocellular carcinoma: a report of the international consensus group for hepatocellular neoplasia. Hepatology 2009;49(2):658–664.

16. Liver Cancer Study Group of Japan. General rules for the clinical and pathological study of primary liver cancer. 3rd ed. Tokyo, Japan: Kanehara, 2010.

17. Vavricka SR, Jung D, Fried M, Grützner U, Meier PJ, Kullak-Ublick GA. The human organic anion transporting polypeptide 8 (SLCO1B3) gene is transcriptionally repressed by hepatocyte nuclear factor 3beta in hepatocellular carcinoma. J Hepatol 2004;40(2):212–218.

18. Gui C, Miao Y, Thompson L, et al. Effect of pregnane X receptor ligands on transport mediated by human OATP1B1 and OATP1B3. Eur J Pharmacol 2008;584(1):57–65.

19. Azuma K, Urano T, Ouchi Y, Inoue S. Vitamin K2 suppresses proliferation and motility of hepatocellular carcinoma cells by activating steroid and xenobiotic receptor. Endocr J 2009;56(7):843–849.

20. Huisse MG, Leclercq M, Belghiti J, et al. Mechanism of the abnormal vitamin K-dependent gamma-carboxylation process in human hepatocellular carcinomas. Cancer 1994;74(5):1533–1541.

21. Saito S, Ojima H, Ichikawa H, Hirohashi S, Kondo T. Molecular background of alpha-fetoprotein in liver cancer cells as revealed by global RNA expression analysis. Cancer Sci 2008;99(12):2402–2409.

22. Lee JS, Heo J, Libbrecht L, et al. A novel prognostic subtype of human hepatocellular carcinoma derived from hepatic progenitor cells. Nat Med 2006;12(4):410–416.

23. Yamashita T, Ji J, Budhu A, et al. EpCAM-positive hepatocellular carcinoma cells are tumor-initiating cells with stem/progenitor cell features. Gastroenterology 2009;136(3):1012–1024.

24. Yamashita T, Forgues M, Wang W, et al. EpCAM and alpha-fetoprotein expression defines novel prognostic subtypes of hepatocellular carcinoma. Cancer Res 2008;68(5):1451–1461.

Liver INTERNATIONAL
OFFICIAL JOURNAL OF THE INTERNATIONAL ASSOCIATION FOR THE STUDY OF THE LIVER

Liver International ISSN 1478-3223

CLINICAL STUDIES

Expression of chondroitin-glucuronate C5-epimerase and cellular immune responses in patients with hepatocellular carcinoma

Eishiro Mizukoshi, Kazumi Fushimi, Kuniaki Arai, Tatsuya Yamashita, Masao Honda and Shuichi Kaneko

Department of Gastroenterology, Graduate School of Medicine, Kanazawa University, Kanazawa, Ishikawa, Japan

Keywords
cancer – CTL – epitope – immunotherapy – peptide vaccine – tumour-associated antigen

Abbreviations
ELISPOT, enzyme-linked immunospot; HCV, hepatitis C virus; HLA, human leucocyte antigen; IFN, interferon; PBMC, peripheral blood mononuclear cells; SART, squamous cell carcinoma antigen recognized by T cells; TIL, tumour infiltrating lymphocytes.

Correspondence
Shuichi Kaneko, MD, Department of Gastroenterology, Graduate School of Medicine, Kanazawa University, Kanazawa, Ishikawa 920-8641, Japan
Tel: + 81-76-265-2230
Fax: + 81-76-234-4250
e-mail: skaneko@m-kanazawa.jp

Received 6 March 2012
Accepted 25 June 2012

DOI:10.1111/j.1478-3231.2012.02853.x

Abstract

Background & Aims: Chondroitin-glucuronate C5-epimerase is an enzyme that converts D-glucuronic acid to L-iduronic acid residues in dermatan sulphate biosynthesis. It is also identified to be a tumour-associated antigen recognized by cytotoxic T cells (CTLs) and its enhanced expression in many cancers has been reported. In the present study, we investigated the usefulness of this molecule as an immunotherapeutic target in hepatocellular carcinoma (HCC). *Methods:* The expression of chondroitin-glucuronate C5-epimerase in hepatoma cell lines and HCC tissues was confirmed by immunofluorescence and immunohistochemical analysis. CTL responses were investigated by several immunological techniques using peripheral blood mononuclear cells (PBMCs) or tumour-infiltrating lymphocytes. To determine the safety of immunotherapy using chondroitin-glucuronate C5-epimerase-derived peptide, 12 patients with HCC were administered s.c. vaccinations of the peptides and analysed. *Results:* Chondroitin-glucuronate C5-epimerase was expressed in HCC cell lines and human tissues including alpha-foetoprotein (AFP)-negative individuals. Chondroitin-glucuronate C5-epimerase-specific CTLs could be generated by stimulating PBMCs of HCC patients with peptides and they showed cytotoxicity against HCC cells expressing the protein. The frequency of CTL precursors investigated by enzyme-linked immunospot (ELISPOT) assay was 0–34 cells/3 × 10^5 PBMCs and the infiltration of interferon-gamma-producing CTLs into the tumour site was confirmed. In the vaccination study, no severe adverse events were observed and the peptide-specific CTLs were induced in 4 of 12 patients tested. *Conclusions:* Chondroitin-glucuronate C5-epimerase is a potential candidate for tumour antigen with immunogenicity and the peptides derived from this antigen could be useful in HCC immunotherapy.

Hepatocellular carcinoma (HCC) is the most frequent primary malignancy of the liver and has gained much clinical interest because of its increasing incidence (1). It is treatable by hepatectomy or percutaneous ablation when the lesion is localized to some extent, and radical therapeutic effects can be obtained when resection or cauterization with a safety margin can be performed (2). However, the recurrence rate is very high (3), because active hepatitis and cirrhosis in surrounding non-tumour liver tissues have the potential to generate HCC de novo.

To protect against recurrence, tumour antigen-specific immunotherapy is an attractive option. Many tumour-associated antigens and their epitopes recognized by cytotoxic T cells (CTLs) have been identified during the last two decades. However, only a few HCC-specific tumour antigens and their antigenic epitopes have been used for human trials (4, 5).

Chondroitin-glucuronate C5-epimerase is an enzyme that converts D-glucuronic acid to L-iduronic acid residues in dermatan sulphate biosynthesis and identical to squamous cell carcinoma antigen recognized by T cells 2 (SART2) (6). It is expressed in many malignant tumour cell lines and various histological types of cancer tissues and function as tumour rejection antigens (7). In addition, peptides containing chondroitin-glucuronate C5-epimerase epitopes are capable of generating CTLs, and therefore, have been used for immunotherapy to treat several kinds of cancers (8, 9). These reports suggest chondroitin-glucuronate C5-epimerase to be useful as a target antigen in HCC immunotherapy. Furthermore, in previous study, we compared T-cell immune responses against the various tumour-associated antigen (TAA)-derived peptides (10). The results of the study showed that CTLs of HCC patients were frequently responsive against a single

chondroitin-glucuronate C5-epimerase-derived peptide. Regarding tumour immunotherapy, it has recently been reported that strong immune responses can be induced at an earlier post-vaccination time using, as peptide vaccines, epitopes that frequently occur in peripheral blood CTL precursors (11). These results also suggest that chondroitin-glucuronate C5-epimerase is useful as a target for HCC immunotherapy.

In the present study, we examined chondroitin-glucuronate C5-epimerase expression in various hepatoma cell lines and HCC tissues of patients, and analysed immune responses to the antigen using peripheral blood mononuclear cells (PBMCs) and tumour-infiltrating lymphocytes (TILs). Furthermore, to investigate the usefulness of HCC immunotherapy targeting chondroitin-glucuronate C5-epimerase, we analysed the safety and cellular immune responses in the patients vaccinated with chondroitin-glucuronate C5-epimerase-derived peptide.

Materials and methods

Patients

Forty-four HLA-A24-positive HCC patients were examined for the expression of chondroitin-glucuronate C5-epimerase and cellular immune responses. Twelve HCC patients were enrolled in vaccination study. Informed consent was obtained from each patient included in the present study and the study protocol conformed to the ethical guidelines of the 1975 Declaration of Helsinki as reflected in a priori approval by the regional ethics committee.

The diagnosis of HCC was histologically confirmed by taking US-guided needle biopsy specimens in 17 cases, surgical resection in nine cases, and autopsy in five cases. For the remaining 13 patients, the diagnosis was based on typical hypervascular tumour staining on angiography in addition to typical findings, which showed hyperattenuated areas in the early phase and hypoattenuation in the late phase on dynamic CT (12). The pathological grading of tumour-cell differentiation was assessed according to the general rules for the clinical and pathological study of primary liver cancer (13). The severity of liver disease was evaluated according to the criteria of Desmet *et al.* using biopsy specimens of liver tissue (14). Eleven normal blood donors and 23 chronic hepatitis C patients (11 cirrhosis) with HLA-A24, who were diagnosed by liver biopsy, served as controls.

Cell lines

Four human hepatoma cell lines (HLF, Hep3B, HLE and Huh7) and Paca-2, which is a pancreatic cancer cell line, were cultured in DMEM (Gibco, Grand Island, NY, USA) with 10% fetal calf serum (FCS) (Gibco). The HLA-A*2402 gene-transfected C1R cell line (C1R-A24) was cultured in RPMI 1640 medium containing 10% FCS and 500 μg/ml of hygromycin B (Sigma, St Louis, MO, USA), and K562 was cultured in RPMI 1640 medium containing 10% FCS (15).

Immunofluorescence and immunohistochemical analysis

The expression of chondroitin-glucuronate C5-epimerase was examined in four different Hepatoma cell lines. A pancreatic cancer cell line (Paca 2) was used as a positive control. They were fixed in acetone with methanol for 5 min and incubated with rabbit anti-human chondroitin-glucuronate C5-epimerase (ProteinTech Group, Inc., Chicago, IL, USA; diluted 1:50) or mouse anti-human AFP (Nichirei Bioscience, Tokyo, Japan) antibody overnight at 4°C. For immunofluorescence analyses, Alexa Fluor 488-conjugated anti-rabbit and anti-mouse IgG (Invitrogen, Tokyo, Japan) were used for chondroitin-glucuronate C5-epimerase and AFP detection respectively.

The expression in HCC tissue was examined in 26 patients. Non-cancerous tissues were also obtained by a paired liver biopsy or surgical resection from the non-neoplastic liver tissue. The tissues were fixed in buffered zinc formalin (Anatech Ltd, Battle Creek, MI, USA), embedded in paraffin, sectioned (at 3 μm), and stained with haematoxylin and eosin. The sections were deparaffinized, treated in a pressure cooker for 1–4 min, and incubated with rabbit anti-human chondroitin-glucuronate C5-epimerase or AFP (DakoCytomation, Inc, Carpinteria, CA, USA) antibody overnight at 4°C. The tissue sections were visualized using the DAKO EnVision^{TM}+ System (DakoCytomation, Inc.). The expression levels were semi-quantitatively classified into four categories (negative to low, moderate and high; negative: no staining, low: <20% of the area stained, moderate: 20%-80% of the area stained, high: >80% of the area stained).

ELISPOT assay

The PBMCs and TILs were isolated as described previously (16). ELISPOT assays were performed as reported previously with the following modifications (16). Three different peptides (Peptide 1; DYSARWNEI, Peptide 2; AYDFLYNYL, Peptide 3; SYTRLFLIL) derived from chondroitin-glucuronate C5-epimerase were used for the detection of CTLs. Negative controls consisted of a HIV envelope-derived peptide (HIVenv$_{584}$) (17). Positive controls consisted of 10 ng/ml of phorbol 12-myristate 13-acetate (PMA, Sigma) or a CMV pp65-derived peptide (CMVpp65$_{328}$) (18). The peptides were synthesized at Sumitomo Pharmaceuticals (Osaka, Japan). The coloured spots were counted with a KS ELISPOT Reader (Zeiss, Tokyo, Japan). The number of specific spots was determined by subtracting the number of spots in the absence of an antigen from the number in its presence. Responses to peptides derived form chondroitin-glucuronate C5-epimerase in HCC

patients were considered positive if the number of specific spots was more than the mean + 3SD of that in normal donors and if the number of spots in the presence of an antigen was at least two-fold greater than the number in its absence. Responses to peptides HIVenv$_{584}$ and CMVpp65$_{328}$ were considered positive if more than 10 specific spots were detected and if the number of spots in the presence of an antigen was at least two-fold that in its absence. ELISPOT assays were also performed in 12 patients whose PBMCs were available for analysis at 2–4 weeks after RFA.

CTL induction and Cytotoxicity assay

Peptide 3 (SYTRLFLIL), which corresponds to HLA-A24-restricted CTL epitope (7, 19), was used to produce chondroitin-glucuronate C5-epimerase-specific T cells. CTLs were expanded from PBMCs as detailed previously (16). C1R-A24 cells and human hepatoma cell lines were used as targets. Cytotoxicity assay was performed by chromium-release assay. Percent cytotoxicity was calculated as previously described (16). For the assay using hepatoma cell lines, cytotoxicity was considered positive when it was higher than that of CTLs against K562 which shows non-specific lysis.

Vaccination study

Twelve HLA-A24-positive HCC patients who were treated by radiofrequency ablation (RFA) and obtained complete necrosis of tumour with safety margin were enrolled in this vaccine study (Trial registration: UMIN000004540). They were vaccinated with peptide 3 (SYTRLFLIL) into the subcutaneous tissue of the armpit 4 weeks after RFA. The peptide utilized in the present study was prepared under conditions of Good Manufacturing Practice (NeoMPS, San Diego, CA, USA). One millilitre of the peptide, which was supplied in vials containing 0.04–4 mg/ml sterile solution, was mixed with an equal volume of incomplete Freund's adjuvant (Montanide ISA-51; Seppic, Paris, France) and emulsified in 5-ml syringes. 1.5 ml of the preparing peptide was injected and the patients received three biweekly vaccinations. Toxicity was assessed every 2 weeks using the National Cancer Institute's Common Toxicity Criteria. To evaluate the immunological effect, ELISPOT assay was performed before and 4 weeks after the final vaccination. Responses to vaccination were considered positive if more than 10 specific spots were detected and if the number of spots after vaccination was at least two-fold than before vaccination. After final vaccination, HCC recurrence was evaluated by dynamic CT or MRI every 3 months.

Statistical analysis

Data are expressed as the mean ± SD. The Mann–Whitney's *U*-test was used for statistical analyses of chondroitin-glucuronate C5-epimerase expression in HCC and non-cancerous liver tissues. The χ^2 test with Yates' correction and the unpaired *t*-test were used for univariate analysis of the effect of variables on the T-cell response against chondroitin-glucuronate C5-epimerase. A level of $P < 0.05$ was considered significant.

Results

Expression of chondroitin-glucuronate C5-epimerase in hepatoma cell lines and HCC tissues

Chondroitin-glucuronate C5-epimerase was expressed in all hepatoma cells (Fig. 1a) and its cellular distribution was cytoplasmic, similar to that in Paca-2, a pancreatic cancer cell line reported to express the protein (7). The expression was observed even in the hepatoma cell lines not expressing AFP, namely HLF and HLE.

The expression of chondroitin-glucuronate C5-epimerase in HCC tissues was examined in 26 HCC patients. A representative result for one HCC patient is shown in Fig. 1b. In this case, the expression of chondroitin-glucuronate C5-epimerase was observed in HCC tissue but not in non-cancerous areas. In addition, AFP was not detected in HCC tissue. To compare the expression levels of this protein between cancerous and non-cancerous tissues, the expression was semi-quantitatively classified into four categories as described in materials and methods, and analysed. The expression levels were higher in HCC tissue than in the non-cancerous tissue ($P < 0.0001$) (Fig. 1c). The expression in liver tissue was also observed in the patients with chronic hepatitis and cirrhosis (Control), however, the expression levels were lower than those in HCC tissue ($P = 0.0137$). The expression of chondroitin-glucuronate C5-epimerase and AFP in HCC tissue was observed in 26 (100%) and 12 (46%) of 26 patients respectively (Fig. 1d). The expression of chondroitin-glucuronate C5-epimerase was observed even in the HCC tissues without AFP expression.

Detection of chondroitin-glucuronate C5-epimerase-specific T cells by IFN-γ ELISPOT analysis

The clinical profiles of the 11 healthy normal donors, 12 patients with chronic hepatitis C, 11 patients with cirrhosis and 44 patients with HCC analysed in the present study are shown in Table 1.

To determine whether a significant number of T cells specifically reacted with the chondroitin-glucuronate C5-epimerase-derived peptides (peptide 1, 2 and 3) in HCC patients, ELISPOT assays were performed using PBMCs from 11 healthy donors (Fig. 2a). The number of specific spots was 1.0 ± 1.3, 1.5 ± 1.3 and 1.0 ± 1.4/3×10^5 PBMCs respectively. Similarly, cells that specifically reacted with the peptides were counted among chronic hepatitis C and cirrhosis patient-derived PBMCs. Regarding a value larger than the mean + 3SD

Liver International (2012)

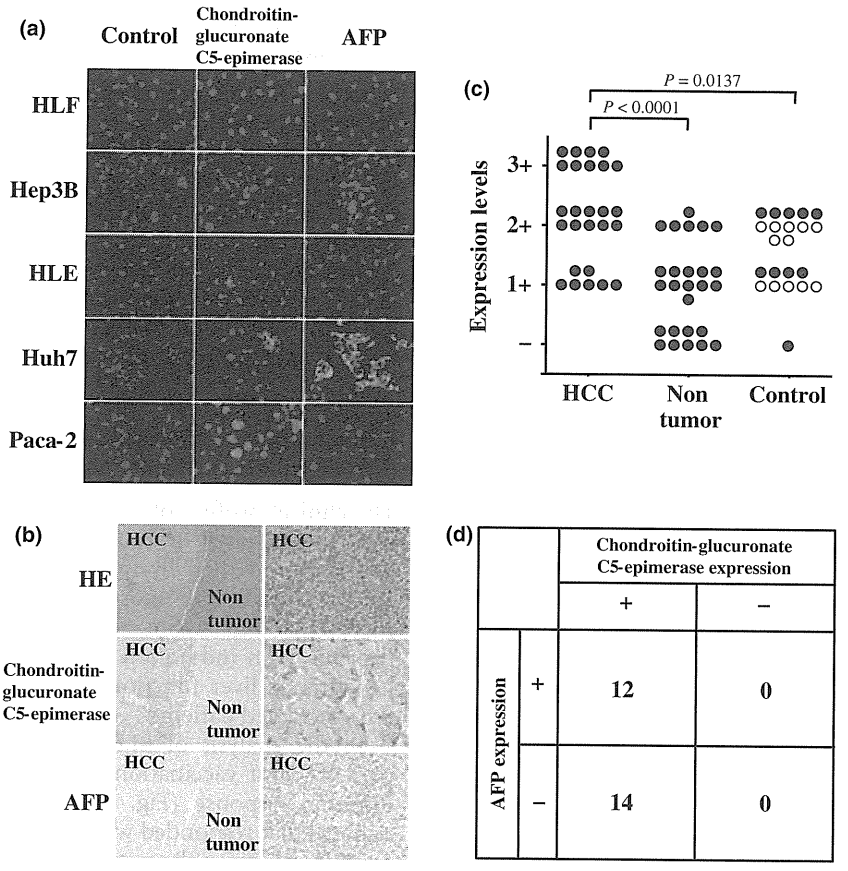

Fig. 1. Expression of chondroitin-glucuronate C5-epimerase. (a) immunofluorescence analysis for the expression of chondroitin-glucuronate C5-epimerase in hepatoma cell lines. Original magnification, ×400. (b) Immunohistochemical analysis for the expression of chondroitin-glucuronate C5-epimerase and AFP in sequential non-cancerous and HCC tissue sections. Original magnification, ×200 (left) and ×400 (right). (c) Analysis of chondroitin-glucuronate C5-epimerase expression levels among the three groups (HCC; tumour tissue in HCC patients, Non-tumour; non-tumour tissue in HCC patients, Control; liver tissue in disease control groups). Closed and open circles show the level of chondroitin-glucuronate C5-epimerase expression in the patients with cirrhosis and chronic hepatitis respectively. (d) The expression of chondroitin-glucuronate C5-epimerase was also compared with AFP expression in HCC tissues.

of the number of T cells that specifically reacted with the peptide in healthy donor-derived PBMCs as a significant response, 1 of 23 (4.3%) patients showed a significant response to each of the chondroitin-glucuronate C5-epimerase-derived peptides (Fig. 2a).

In the same analysis of HCC patients, 10.8, 16.2 and 27.0% of the patients showed significant responses to peptide 1, 2 and 3 respectively (Fig. 2b). A significant response specific to $CMVpp65_{328}$ was detected in 36.4%, 34.8% and 45.9% of healthy donors, disease control groups and HCC patients, respectively, with no significant difference among the three groups. On the other hand, no significant response to $HIVenv_{584}$ was observed in all groups.

To clarify the clinical characteristics of chondroitin-glucuronate C5-epimerase-specific T-cell responses in HCC patients, the clinical background was compared between patients who showed positive responses to chondroitin-glucuronate C5-epimerase-derived peptides and those who did not. The clinical features of both groups were not statistically different in terms of age, gender, serum AFP levels, differentiation of HCC, tumour multiplicity, vascular invasion, TNM factors and stages, histology of the non-tumour liver, liver function and the type of viral infection (Table 2). Chondroitin-glucuronate C5-epimerase-specific T cells had been generated even in the early stages of HCC.

Next, to examine the existence of chondroitin-glucuronate C5-epimerase-specific T cells among TILs, we performed a similar analysis in another seven patients from whom samples of both PBMCs and TILs could be obtained. In the assay using PBMCs and TILs, four of seven (57.1%) and five of seven (71.4%) patients, respectively, showed significant responses to chondroitin-glucuronate C5-epimerase-derived peptide (peptide 3) (Fig. 3a). A positive T-cell response in TILs was observed even in one patient without a positive T-cell response in PBMCs (patient 39).

Table 1. Characteristics of the patients studied

Clinical diagnosis	No. of patients	gender M/F	Age (yr) Mean ± SD	ALT (IU/L) Mean ± SD	AFP (ng/ml) Mean ± SD	Aetiology (B/C/Others)	Child-Pugh (A/B/C)	Diff. degree[a] (wel/mod /por/ND)	Tumour size[b] (large/small)	Tumour multiplicity (multiple/solitary)	Vascular Invasion (+/−)	TNM stage (I/II/IIIA/IIIB/ IIIC/IV)
Normal donors	11	8/3	35 ± 2	ND	ND	ND	ND	ND	ND	ND	ND	ND
Chronic hepatitis	12	7/5	54 ± 11	104 ± 119	12 ± 4	0/12/0	12/0/0	ND	ND	ND	ND	ND
Liver cirrhosis	11	5/6	60 ± 11	83 ± 73	79 ± 140	1/7/3	6/5/0	ND	ND	ND	ND	ND
HCC	44	35/9	66 ± 8	67 ± 32	1629 ± 7874	8/34/2	28/14/2	11/17/3/13	29/15	25/19	12/32	13/17/5/ 1/2/6

[a]Histological degree of HCC; wel: well-differentiated, mod: moderately differentiated, por: poorly differentiated, ND: not determined.
[b]Tumour size was divided into either 'small' ($\leq$ 2 cm) or 'large' (>2 cm).

Cytotoxic activity of chondroitin-glucuronate C5-epimerase-specific CTLs against hepatoma cell lines

Whether the chondroitin-glucuronate C5-epimerase-derived peptides used were capable of generating peptide-specific CTLs from PBMCs was investigated in 18 HCC patients. The CTLs specific to chondroitin-glucuronate C5-epimerase could be induced in 8 of 18 (44.4%) patients (Fig. 3b and c). They exhibited cytotoxicity against hepatoma cell lines with the HLA-A24 molecule and expression of chondroitin-glucuronate C5-epimerase, that correspond to HLF and HLE, but not against Hep3B and Huh7 cells without HLA-A24 (Fig. 3d).

Clinical safety of chondroitin-glucuronate C5-epimerase-derived peptide and its immunological effects

The clinical profiles of the 12 HCC patients with vaccination are shown in Table 3. The treatment was well-tolerated and there were no treatment-related serious adverse events. The most common adverse event was grade 1 injection-site reaction manifesting as pain, pruritus, skin induration and rubor. The worsening of hepatitis or liver function was not observed in any of the vaccinated patients.

In the analysis of ELISPOT assay using PBMCs of patients with vaccination, 4 patients demonstrated an immune response (Fig. 4a and Table 3). All of the patients that responded were immunized with 3.0 mg of peptide. None of the patients immunized with 0.03 or 0.3 mg of peptide showed an enhancement of peptide-specific immune response. The enhancement of immunological response to $HIVenv_{584}$ and $CMVpp65_{328}$ was not observed in any patients except patient A2.

To examine whether similar occurs for the immune response in HCC patients with only RFA, we analysed chondroitin-glucuronate C5-epimerase-derived peptide-specific T-cell responses in 12 HCC patients without vaccination, whose PBMCs were available for analysis at 2–4 weeks after RFA. In this analysis, we observed an increase of the frequency of chondroitin-glucuronate C5-epimerase-derived peptide-specific T cells in 2 of 12 patients (Fig. 4b). The frequency of the patients who showed an increase in the number of chondroitin-glucuronate C5-epimerase-derived peptide-specific T cells was higher in the patients with vaccination of 3 mg of peptide (66.7%) than in those without vaccination (16.7%).

Finally, we examined the HCC recurrence rate after RFA between the patients with and without the peptide-specific CTL response to examine the clinical effect of an increase of chondroitin-glucuronate C5-epimerase-derived peptide-specific CTLs after vaccination. In the analysis, the recurrence rate in the patients with an increase in the peptide-specific CTLs after vaccination (two of four patients, 50%) was lower than that in the patients without immune response (six of eight patients, 75%) at 300 days after RFA, although there was no sta-

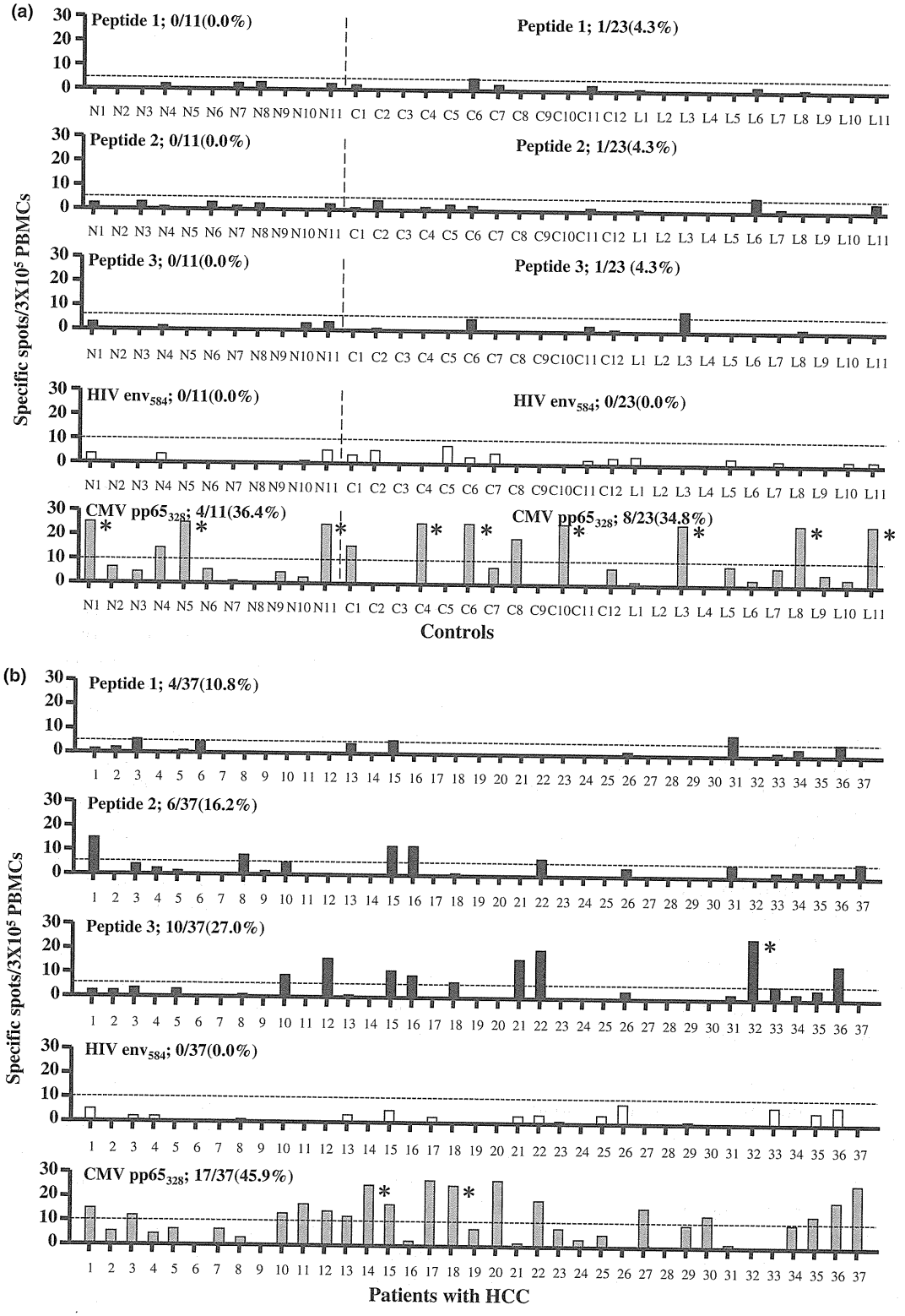

Fig. 2. Immune responses of chondroitin-glucuronate C5-epimerase-specific T cells. (a) IFN-γ ELISPOT assay of PBMCs to chondroitin-glucuronate C5-epimerase-derived peptides (peptides 1, 2 and 3: solid bars) or control peptides (peptides HIVenv$_{584}$ and CMVpp65$_{328}$: open and grey bars respectively) in normal donors and disease control groups. "N" denotes normal donors. "C" denotes the patients with chronic hepatitis. "L" denotes the patients with cirrhosis.% shows the ratio of the patients who showed positive responses. *denotes more than 30 specific spots. (b) IFN-γ ELISPOT assay in HCC patients. *denotes more than 30 specific spots.

Table 2. Univariate analysis of the effect of variables on the T-cell response against chondroitin-glucuronate C5-epimerase

	Patients with positive T-cell response	Patients without positive T-cell response	*P*-value[a]
No. of patients	15	22	
Age (years)[b]	64.6 ± 9.8	68.7 ± 5.9	NS
gender(M/F)	14/1	15/7	NS
AFP (ng/ml)	3569.7 ± 13070.0	580.7 ± 2394.2	NS
Diff. degree of HCC (well/moderate or poor/ND)[c]	3/7/5	8/6/8	NS
Tumour multiplicity (multiple/solitary)	10/5	13/9	NS
Vascular invasion (+/-)	5/10	6/16	NS
TNM factor			
(T1/T2–4)	4/11	8/14	NS
(N0/N1)	14/1	22/0	NS
(M0/M1)	13/2	20/2	NS
TNM stage (I/II–IV)	4/11	8/14	NS
Histology of non-tumour liver (LC/Chronic hepatitis)	12/3	20/2	NS
Liver function (Child A/B/C)	11/4/0	13/7/2	NS
Aetiology (HCV/HBV/Others)	11/3/1	20/1/1	NS
T-cell response against to CMV $pp65_{328}$ (+/-)	9/6	9/13	NS

[a]NS: not significant.
[b]Data are expressed as the mean ± SD.
[c]ND: not determined.

tistical significance owing to the small number of patients.

Discussion

Many tumour-associated antigens and their epitopes capable of inducing HLA-class I-restricted CTLs have been identified in various cancers. Some of the epitopes have been under investigation for the treatment of cancer, with major clinical responses in some trials (11, 20–22).

With regard to immunotherapy for HCC, AFP is considered a useful tumour-associated antigen and AFP-derived peptides have actually been used in clinical trials (5, 23–25). However, in general, the production of AFP depends on the size of the tumour, with AFP expressed in only 0–40% of HCCs less than 30 mm in size (26). Therefore, for immunotherapy for HCC in cases where AFP is not expressed in tumour tissue, it is necessary to identify other tumour-associated antigens.

In the present study, the expression of chondroitin-glucuronate C5-epimerase was observed in all of the HCC tissues examined and independent of differential degree, size, TNM stage and the expression of AFP in the tumour. These results suggest the advantage of this antigen as a target for immunotherapy of HCC.

On the other hand, the expression of this protein was also observed in non-cancerous tissue of HCC patients, although less frequently and at lower levels than in HCC tissue. Our results are consistent with the recent finding that chondroitin-glucuronate C5-epimerase is expressed in some normal tissues including liver tissue (6). Such results imply that immunotherapy targeting chondroitin-glucuronate C5-epimerase may have adverse effects on liver tissue expressing the protein. Therefore, we next examined the existence and specificity of chondroitin-glucuronate C5-epimerase-specific CTLs in HCC patients.

The presence of chondroitin-glucuronate C5-epimerase-recognizing CTLs has been reported as SART2-specific CTLs in lung, gastric and pancreatic cancer patients (7, 27, 28). However, to our knowledge, there has been no report of the presence of chondroitin-glucuronate C5-epimerase-specific CTLs in HCC patients except our recent study using only one SART2-derived peptide (10). In this study, we used three different HLA-A24 restricted peptides which were previously identified and derived from naturally processed squamous cell carcinoma antigen. The HLA-A24 allele is found in 60% of Japanese (29), and therefore, to use HLA-A24-restricted peptides has the advantage of analysing CTL responses to tumour-associated antigens in Japanese patients.

We showed that chondroitin-glucuronate C5-epimerase-specific CTLs could be generated by stimulating PBMCs with peptides, and the CTLs were cytotoxic to hepatoma cell lines. Chondroitin-glucuronate C5-epimerase-specific immune responses were observed frequently only in HCC patients and the frequency of CTLs was higher in HCC patients than control groups, indicating that the immune responses are specific to HCC. Furthermore, the CTLs were also detected among TILs, suggesting that they infiltrate the tumour. Based on these findings, we confirmed that chondroitin-glucuronate C5-epimerase-specific CTL precursors exist in HCC patients and the immune responses are specific for HCC.

In previous study, we reported that the frequency of TAA-derived peptide-specific CTLs in HCC patients was 0–92 cells/3 × 10^5 PBMCs and the frequency of the

Liver International (2012)